2020

Effect of Subsurface Microseismicity on the Motion of Surrounding Dispersed Droplets: Supporting Information

Chao Zeng

Wen Deng
Missouri University of Science and Technology, wendeng@mst.edu

Effect of Subsurface Microseismicity on the Motion of Surrounding Dispersed Droplets: Supporting Information

Abstract

The human-induced seismicity has called substantial attention in recent years. The effect of seismicity on the subsurface structure has been extensively studied. However, the effect of seismicity, especially those microseismicity, on surrounding immiscible fluids is rarely investigated. In porous media with two or more immiscible fluids, different amplitudes of vibration induced by seismicity have distinct effects on the dynamic behavior of fluids. Three types of pore-scale models are prevalent in the analysis of the motion of immiscible droplets. The underlying assumptions and accuracy of these models are compared in this study in both frequency domain and time domain. The frequency domain analysis shows that the resonance can be addressed in all of three models, but the frequency response curves present significant differences. These differences are attributed to the missing physics considered in some models. The time domain analysis in both small-amplitude oscillation and large-amplitude oscillation is performed. The nonlinear feature in large-amplitude oscillation is attributed to the constricted geometry of capillary tube. The momentum balance model is identified as so-far the most accurate oscillatory model by the comparison with computational fluid dynamics simulations. In addition, the potential approach to incorporate this pore-scale model in seismic wave attenuation analysis is found possible. The frequency correction function and structural factor are calculated to embed the momentum balance model into *Biot* 's poroelastic model. The resonance of dispersed phase can also be addressed theoretically in porous media of random packed spheres.

Disciplines

Geophysics and Seismology | Geotechnical Engineering

[Journal of Geophysical Research: Solid Earth]

Supporting Information for

Effect of Subsurface Microseismicity on the Motion of Surrounding Dispersed Droplets

Chao Zeng[1], Wen Deng[1*]

1 Department of Civil, Architectural and Environmental Engineering, Missouri University of Science and Technology, Rolla, Missouri, USA 65409

* Corresponding author. Tel: +1 573 341 4484. E-mail address: wendeng@mst.edu

Contents of this file

Text S1.

Details of Three Models for Resonance Analysis

Pressure balance model

Governing equation

The model geometry shown in Figure 1c was used to establish theoretical model. The capillary tube vibrates with the same frequency as exerted seismic wave. In a response to the vibration, the viscous pressure drops in three fluid slugs 1, 2, and 3 (Figure 1c) are equal to the capillary pressure variation. The governing equation is:

$$\int_s^h \nabla P_n^{vis}(t)dx + \int_{L_1}^s \nabla P_w^{vis}(t)dx + \int_h^{L_2} \nabla P_w^{vis}(t)dx = \Delta P_c(t) - \Delta P_c(0) \quad \text{(S1)}$$

where ∇P_n^{vis} and ∇P_w^{vis} denote viscous gradient in nonwetting phase and wetting phase, respectively. $\Delta P_c(t)$ and $\Delta P_c(0)$ denote capillary pressure difference at two meniscus at arbitrary time t and initial equilibrium state. On the left-hand side, the terms represent viscous pressure drops in three slugs respectively. On the right-hand side, it represents the temporal variation of the capillary pressure difference in oscillation.

Linear analysis

In the circumstance of small oscillation of the droplet, the linearized approximation is applicable and the validity for this approximation will be discussed later. In addition, the droplet is under forced vibration stimulated by the external seismic excitation. Equation (9) can be expressed as a complex form:

$$a(t) = a(\omega)e^{-i\omega t} \tag{S2}$$

The imaginary part of $a(t)$ is the real acceleration on the tube. $a(\omega)$ is used to generalize the seismic waves with multiple frequencies. In this study, $a(\omega)=A$.

Therefore, the transient positions of h and s can be expressed as:

$$h(t) = h_0 + \Delta h \cdot e^{-i\omega t} \tag{S3}$$

$$s(t) = s_0 + \Delta s \cdot e^{-i\omega t} \tag{S4}$$

The rigorous expression for the small displacement is: $\Delta h/h_0 \ll 1$ and $\Delta s/s_0 \ll 1$. Considering the relation of Δs and Δh by the volume conservation in equation (7), Δs can be expressed as (see **S2**):

$$\Delta s = \Upsilon(\beta, \Lambda, x^*) \cdot \Delta h \tag{S5}$$

where $\beta = L/r_{min}$, $\Lambda = r_{max}/r_{min}$, $x^* = x/L$, $\Upsilon(\beta, \Lambda, x^*)$ refers to equation (S43).

In addition, based on equation (S3), the velocity and acceleration can be formulated as:

$$\frac{dh}{dt} = -i\omega\Delta h \cdot e^{-i\omega t} \tag{S6}$$

$$\frac{d^2h}{dt^2} = -\omega^2\Delta h \cdot e^{-i\omega t} \tag{S7}$$

The external pressure difference and capillary pressure difference are combined together. The linearized approximation is applied on equation (4), and the simplified form of pressure difference is (see **S3**):

$$\Delta P_e - \Delta P_c = -2\sigma \frac{f(\beta,\Lambda,x^*)}{r_{min}^2}\Delta h \cdot e^{-i\omega t} \tag{S8}$$

The specific form of $f(\beta, \Lambda, x^*)$ refers to equation (S48).

It is noted that $\Delta P_c(0) = \Delta P_e$ for this study due to initially stationary state of the nonwetting phase. The detailed derivation refers to their work [Hilpert et al., 2000]. Only the final governing equation is presented in this study. The transient motion of nonwetting droplet follows:

$$\rho_n\omega^2\lambda^2(h)\Delta h\int_s^h\frac{1}{\lambda^2(\xi)h\left(\frac{\omega}{\omega_c^n}\right)}d\xi+\rho_w\omega^2\lambda^2(h)\Delta h\int_{L_1}^s\frac{1}{\lambda^2(\xi)h\left(\frac{\omega}{\omega_c^w}\right)}d\xi$$
$$+\rho_w\omega^2\lambda^2(h)\Delta h\int_h^{L_2}\frac{1}{\lambda^2(\xi)h\left(\frac{\omega}{\omega_c^w}\right)}d\xi$$
$$=2\sigma\left[\frac{1}{\lambda_{men}(h)}-\frac{1}{\lambda_{men}(h_0)}\right]+\rho_n a(\omega)(h-s)$$
$$+\rho_w a(\omega)(s-L_1+L_2-h) \tag{S9}$$

where Δh is the displacement of the front meniscus, the same as that in equation (S3); This equation is formulated in the frequency domain. $h\left(\frac{\omega}{\omega_c^k}\right)$ is expressed as:

$$h\left(\frac{\omega}{\omega_c^k}\right)=-\frac{J_2\left(\sqrt{i^3\omega/\omega_c^k}\right)}{J_0\left(\sqrt{i^3\omega/\omega_c^k}\right)}\quad(k=n,w) \tag{S10}$$

$$\omega_c^k=\frac{\mu_k}{\rho_k\lambda^2(x)}(k=n,w) \tag{S11}$$

where J_0 and J_2 denote Bessel function of order 0 and 2, respectively. Equation (S11) represents the characteristic frequency for the nonwetting droplet $(k=n)$ and wetting fluid $(k=w)$. ω/ω_c^k is the dimensionless frequency.

In addition, the *h* and *s* in other terms can be treated as initial values in the context of small oscillation. The simplified equation is:

$$[\rho_n(h_0-s_0)+\rho_w(s_0-L_1+L_2-h_0)]a(\omega)=\left\{\rho_n\lambda^2(h_0)\int_{s_0}^{h_0}\frac{1}{\lambda^2(\xi)h\left(\frac{\omega}{\omega_c^n}\right)}d\xi+\right.$$
$$\left.\rho_w\lambda^2(h_0)\int_{L_1}^{s_0}\frac{1}{\lambda^2(\xi)h\left(\frac{\omega}{\omega_c^w}\right)}d\xi+\rho_w\lambda^2(h_0)\int_{h_0}^{L_2}\frac{1}{\lambda^2(\xi)h\left(\frac{\omega}{\omega_c^w}\right)}d\xi\right\}\omega^2\Delta h-2\sigma\frac{f(\beta,\Lambda,x^*)}{r_{min}^2}\Delta h \tag{S12}$$

Frequency response function

In harmonic oscillator, the frequency response function can characterize the oscillatory properties, i.e. damping ratio, resonance frequency, and output displacement magnification. By an analogy, to characterize the oscillation of the droplet in this system, the frequency response function is defined as the ratio of the output displacement to the input acceleration amplitude in a dimensionless form:

$$\chi(\omega)=-\frac{\Delta h}{a(\omega)}(\omega_c^n)^2 \tag{S13}$$

where the negative sign applies in the calculation of χ(ω) which is the acceleration of tube, and the acceleration imposed on the nonwetting fluid is the negative of this value. The ω_c^n is the characteristic frequency of the nonwetting phase as defined in equation (S11), in order to non-dimensionalize $\chi(\omega)$.

By reorganizing equation (S12) and substituting into equation (S13), the frequency response function can be obtained as:

$$\chi^I(\omega) = \frac{\rho_n(h_0 - s_0) + \rho_w(s_0 - L_1 + L_2 - h_0)}{2\sigma\frac{f(\beta,\Lambda,x^*)}{r_{min}^2(\omega_c^n)^2} - \frac{\omega^2}{(\omega_c^n)^2}\left[\rho_n\lambda^2(h_0)\int_{s_0}^{h_0}\frac{1}{\lambda^2(\xi)h\left(\frac{\omega}{\omega_c^n}\right)}d\xi + \rho_w\lambda^2(h_0)\int_{L_1}^{s_0}\frac{1}{\lambda^2(\xi)h\left(\frac{\omega}{\omega_c^w}\right)}d\xi + \rho_w\lambda^2(h_0)\int_{h_0}^{L_2}\frac{1}{\lambda^2(\xi)h\left(\frac{\omega}{\omega_c^w}\right)}d\xi\right]} \quad \text{(S14)}$$

The Roman numeral "I" was used as the superscript to differentiate other frequency response functions which will be used in later part. For short abbreviation, the pressure balance model is referred to as model I thereafter.

As an analogy to the second-order harmonic oscillator system, the natural frequency of the droplet is:

$$\omega_0 = \sqrt{\frac{2\sigma f(\beta,\Lambda,x^*)}{[\rho_n(h_0 - s_0) + \rho_w(s_0 - L_1 + L_2 - h_0)]r_{min}^2}} \quad \text{(S15)}$$

The dimensionless natural frequency is:

$$X_0 = \frac{\omega_0}{\omega_c^n} \quad \text{(S16)}$$

It is noted that the dimensionless form of X_0^2 is:

$$X_0^2 = \frac{r_{min}}{Oh^2}\frac{2f(\beta,\Lambda,x^*)}{(h_0 - s_0) + a_\rho(s_0 - L_1 + L_2 - h_0)} \quad \text{(S17)}$$

where $a_\rho = \rho_w/\rho_n$ is the density ratio of the wetting phase to the nonwetting phase. Oh is the Ohnesorge number that relates the viscous forces to inertial and surface tension forces. The natural frequency is function of geometry in the system and fluid properties.

The dimensionless excitation frequency in the nonwetting phase and wetting phase were defined as:

$$X_n = \frac{\omega}{\omega_c^n} \quad \text{(S18)}$$

$$X_w = \frac{\omega}{\omega_c^w} \quad \text{(S19)}$$

By using equations (S17), (S18) and (S19), equation (S14) can be reformulated as:

$$\chi^I(\omega) = \frac{1}{X_0^2 - X_n^2\left[\frac{\lambda^2(h_0)\int_{s_0}^{h_0}\frac{1}{\lambda^2(\xi)h\left(\frac{\omega}{\omega_c^n}\right)}d\xi + a_\rho\lambda^2(h_0)\int_{L_1}^{s_0}\frac{1}{\lambda^2(\xi)h\left(\frac{\omega}{\omega_c^w}\right)}d\xi + a_\rho\lambda^2(h_0)\int_{h_0}^{L_2}\frac{1}{\lambda^2(\xi)h\left(\frac{\omega}{\omega_c^w}\right)}d\xi}{(h_0 - s_0) + a_\rho(s_0 - L_1 + L_2 - h_0)}\right]} \quad \text{(S20)}$$

Force balance model

Governing equation

For a nonwetting droplet driven by a constant background pressure gradient ∇P, the droplet would be trapped near the pore throat as shown in Figure 1c. In the steady state, this constant pressure gradient balances the initial capillary force difference as:

$$\nabla P(h_0 - s_0) = 2\sigma\left[\frac{1}{\lambda_{men}(s_0)} - \frac{1}{\lambda_{men}(h_0)}\right] \tag{S21}$$

In the presence of externally oscillatory excitation, the equation of motion of the droplet is formulated as:

$$\rho_n \frac{d^2h}{dt^2} - \frac{2\sigma}{h_0 - s_0}\left[\frac{1}{\lambda_{men}(s)} - \frac{1}{\lambda_{men}(h)}\right] + \rho_n a(t) + \nabla P + \frac{16\mu_n}{(r_{max}+r_{min})^2}\frac{dh}{dt} = 0 \tag{S22}$$

Some symbols of variables in their model are converted to make them consistent within this study, without change of physical meaning. In their work [Beresnev and Deng, 2010], the motion of droplet is depicted by the contact line of rear meniscus. The constant length of droplet in constricted capillary tube is assumed. To be consistent with other two models, the position h of front meniscus contact line is used to express the equation. In addition, the water film is not presented in equation (S22) compared to equation (6) in Beresnev and Deng [2010]. On the left-hand side, the terms represent inertial force, volume-averaged capillary force, oscillatory body force, constant background pressure gradient, and viscous force, respectively. This equation is a second-order nonlinear ordinary differential equation (ODE) of *h*. The numerical solution was sought to obtain the transient motion of the droplet in a response to the vibration excitation. To seek the analytical solution of oscillatory characteristics, the linear approximation is required.

Linear analysis

It is assumed that the oscillation of the droplet is small enough to linearize equation (S22). Equations (S2), (S3), (S4), (S5), (S6), and (S7) are also used in this analysis. By applying these equations to equations (S21) and (S22), the linearized form is:

$$-\rho_n\omega^2\Delta h + \frac{2\sigma}{h_0 - s_0}\frac{f(\beta,\Lambda,x^*)}{r_{min}^2}\Delta h + \rho_n a(\omega) - \frac{16\mu_n}{(r_{max}+r_{min})^2} i\omega\Delta h = 0 \tag{S23}$$

It is noted that the viscous force used to derive equation (S23) is based on the Poiseuille flow profile, but the derivation of other two models is based on the oscillatory flow profile as introduced in equation (11). The effect of this distinction will be analyzed on the damping and the phase angle of the droplet oscillation.

Frequency response function

To characterize the oscillation of droplet in the system, the frequency response function defined in equation (S13) is also employed. By substituting equation (S23) into equation (S13), we got the frequency response function as:

$$\chi^{II}(\omega) = \frac{1}{\frac{2\sigma}{\rho_n(h_0 - s_0)}\frac{f(\beta,\Lambda,x^*)}{(\omega_c^n)^2 r_{min}^2} - \frac{\omega^2}{(\omega_c^n)^2}\left[1 + \frac{16\mu_n}{\rho_n(r_{max}+r_{min})^2}\frac{i}{\omega}\right]} \tag{S24}$$

This force balance model is referred to as model II in the following discussion. Similar to the derivation process used above, the natural frequency of the droplet is defined as:

$$\omega_0^{II} = \sqrt{\frac{2\sigma}{\rho_n(h_0 - s_0)}\frac{f(\beta,\Lambda,x^*)}{r_{min}^2}} \tag{S25}$$

The dimensionless natural frequency is:

$$X_0^{II} = \frac{\omega_0^{II}}{\omega_c^n} \tag{S26}$$

The dimensionless form of $(X_0^{II})^2$ is:

$$(X_0^{II})^2 = \frac{1}{Oh^2}\frac{2f(\beta,\Lambda,x^*)}{\hat{h}_0 - \hat{s}_0} \tag{S27}$$

By using equation (S26), the frequency response function in equation (S24) can be expressed as:

$$\chi^{II}(\omega) = \frac{1}{(X_0^{II})^2 - (X_n^{II})^2\left[1+\frac{16}{(\Lambda+1)^2}\frac{i}{X_n^{II}}\right]} \tag{S28}$$

Momentum balance model

Governing equation

The momentum balance equation of fluid flow was employed to describe the dynamic behavior of the nonwetting droplet in a response to the oscillatory force. With the lubrication approximation by assuming the slope of the wall is gentle, the flow has only longitudinal component as present in equation (11). The nonwetting droplet can be treated as a moving boundary control volume. The longitudinal component of momentum balance equation can be given as [Deng and Cardenas, 2013]:

$$\rho_n \frac{d}{dt}\int_V \bar{u}_n dV = F_x + F_p + F_a + P_u A_u - P_d A_d \tag{S29}$$

The left-hand side specifies the rate of change of momentum within the control volume *V*; $\bar{u}_n$ is the cross-sectional mean velocity of the nonwetting fluid. On the right-hand side, F_x is the viscous force of nonwetting fluid; F_p is the pressure force along the wall; F_a is the oscillatory fictitious force; P_u and P_d are the pressure at the upstream and downstream menisci of nonwetting droplet; A_u and A_d are the cross-sectional areas at the three phase contact line of upstream and downstream menisci.

The detailed calculation of each term refers to their work [Deng and Cardenas, 2013]. In their study, the thickness of water film is considered in the governing equation. This thickness is set a zero in this simplified form. Only the final governing equation is displayed. The transient motion of the nonwetting droplet follows:

$$\rho_n\left[\frac{2}{3}\lambda(s) + h - s + \lambda(h)g(h)\frac{3+g^2(h)}{6}\right]\frac{d^2h}{dt^2} + \rho_n\left[1 - \frac{\lambda^2(h)}{\lambda^2(s)}\right]\left(\frac{dh}{dt}\right)^2 + 2\rho_n\omega \cdot int1(h)\frac{dh}{dt}$$

$$= \Delta P_e - \Delta P_c - \rho_w\omega\lambda^2(h)\frac{dh}{dt}\left[\int_{L_1}^{s}\frac{1}{\lambda^2(x)\cdot Re\left\{i\cdot h\left(\frac{\omega}{\omega_c^w}\right)\right\}}dx + \int_h^{L_2}\frac{1}{\lambda^2(x)\cdot Re\left\{i\cdot h\left(\frac{\omega}{\omega_c^w}\right)\right\}}dx\right]$$

$$-2\rho_n\omega \cdot int3(h)\frac{dh}{dt} - \rho_n a(t)(h-s) - \rho_w a(t)(s-L_1+L_2-h) \tag{S30}$$

where the forms of $int1(h)$, $int2(h)$, $int3(h)$ and $h\left(\frac{\omega}{\omega_c^w}\right)$ are given as below, respectively:

$$int1(h) = Re\left\{\int_s^h \frac{i^{3/2}}{\sqrt{\omega/\omega_c^n}} \frac{J_1\left(\sqrt{i^3\omega/\omega_c^n}\right)}{J_2\left(\sqrt{i^3\omega/\omega_c^n}\right)} d\xi\right\} \tag{S31}$$

$$int2(h) = Re\left\{\int_s^h \frac{i}{\lambda^2(\xi)h\left(\frac{\omega}{\omega_c^n}\right)} d\xi\right\} \tag{S32}$$

$$int3(h) = \int_s^h int2(\xi)\lambda(\xi)\lambda'(\xi)d\xi \tag{S33}$$

Equation (S30) is highly nonlinear ODE of h in the time domain. This nonlinear equation depicts the oscillation of the nonwetting droplet. Most existing theoretical models are constrained to small oscillation, but this model can also capture large oscillation and mobilization of the droplet [Deng and Cardenas, 2013]. This equation was numerically solved to analyze the mobilization and the small oscillation of the nonwetting droplet at the constriction. Even though the governing equation (S30) has been greatly simplified compared to computational fluid dynamics (CFD) simulations, the characteristics of oscillation is still implicit in this equation. For potential applications of the proposed theoretical model, an explicit form of the oscillatory characteristics is always favorable. In this study, linearized approximation is applied on the equation (S30) to simplify this formula.

Linear analysis

In equation (S30), the second term in the left-hand side has a second-order of *Δh* which can be neglected in this study. By substituting equations (S3), (S6), (S7) and (S8) to equation (S30), we can get:

$$[\rho_n(h_0-s_0)+\rho_w(s_0-L_1+L_2-h_0)]a(\omega) = \left\{\rho_w\lambda^2(h_0)\left(\int_{L_1}^{s} \frac{1}{\lambda^2(\xi)\cdot\hat{h}\left(\frac{\omega}{\omega_c^w}\right)} d\xi + \int_h^{L_2} \frac{1}{\lambda^2(\xi)\cdot\hat{h}\left(\frac{\omega}{\omega_c^w}\right)} d\xi\right) + 2\rho_n int3(h_0) + \rho_n\left[\frac{2}{3}\lambda(s_0) + h_0 - s_0 + \lambda(h_0)g(h_0)\frac{3+g^2(h_0)}{6}\right] + 2\rho_n int1(h_0)\right\}\omega^2\Delta h - 2\sigma\frac{f(\beta,\Lambda,x^*)}{r_{min}^2}\Delta h \tag{S34}$$

Equation (S34) is expressed in the frequency domain. The left-hand side term represents driving force per volume in the fluid system. The right-hand side terms represent the inertial force, damping force and restoring force per volume, respectively.

Frequency response function

By reorganizing equation (S34) and then substituting into equation (S13), the frequency response function is:

$$\chi^{III}(\omega) = \frac{\rho_n(h_0 - s_0) + \rho_w(s_0 - L_1 + L_2 - h_0)}{2\sigma\frac{f(\beta,\Lambda,x^*)}{(\omega_c^n)^2 r_{min}^2} - \frac{\omega^2}{(\omega_c^n)^2}\left[\rho_n\lambda^2(h_0)\left(\int_{L_1}^{s_0}\frac{1}{\lambda^2(\xi)\cdot\hat{h}\left(\frac{\omega}{\omega_c^w}\right)}d\xi + \int_{h_0}^{L_2}\frac{1}{\lambda^2(\xi)\cdot\hat{h}\left(\frac{\omega}{\omega_c^w}\right)}d\xi\right) + 2\rho_n int3(h_0) + \rho_n\left[\frac{2}{3}\lambda(s_0) + h_0 - s_0 + \lambda(h_0)g(h_0)\frac{3+g^2(h_0)}{6}\right] + 2\rho_n int1(h_0)\right]} \tag{S35}$$

Momentum balance model is referred as model III in following analysis. It shows that model III has the same natural frequency as ω_0 in equation (S15), which is different from model II. By the non-dimensionalization, the frequency response function in equation (S35) can be expressed as:

$$\chi^{III}(\omega) = \frac{1}{X_0^2 - X_n^2\left[\frac{a_\rho\lambda^2(h_0)\left(\int_{L_1}^{s_0}\frac{1}{\lambda^2(\xi)\cdot h\left(\frac{\omega}{\omega_c^w}\right)}d\xi + \int_{h_0}^{L_2}\frac{1}{\lambda^2(\xi)\cdot h\left(\frac{\omega}{\omega_c^w}\right)}d\xi\right) + 2int3(h_0) + \left[\frac{2}{3}\lambda(s_0) + h_0 - s_0 + \lambda(h_0)g(h_0)\frac{3+g^2(h_0)}{6}\right] + 2int1(h_0)}{(h_0 - s_0) + a_\rho(s_0 - L_1 + L_2 - h_0)}\right]} \tag{S36}$$

Text S2.

Volume of Droplet

The volume of droplet at initial stationary state is (see equation 7):

$$V_0 = \frac{2\pi}{3}r_{max}^3 + \pi r_{max}^2(-L - s_0) + \pi\int_{-L}^{h_0}\lambda^2(x)dx + \frac{\pi H(h_0)}{6}[3\lambda^2(h_0) + H^2(h_0)] \tag{S37}$$

The displacement of *h* and *s* in transient state can be expressed as:

$$h(t) = h_0 + \Delta h \tag{S38}$$

$$s(t) = s_0 + \Delta s \tag{S39}$$

Then, the volume of droplet in transient state can be formulated as:

$$V = \frac{2\pi}{3}r_{max}^3 + \pi r_{max}^2(-L - s_0 - \Delta s) + \pi\int_{-L}^{h_0+\Delta h}\lambda^2(x)\,dx + \frac{\pi H(h_0+\Delta h)}{6}[3\lambda^2(h_0 + \Delta h) + H^2(h_0 + \Delta h)] \tag{S40}$$

For the incompressibility of nonwetting droplet, the volume is conserved. Thus, the displacement at the rear meniscus is:

$$\Delta s = \frac{1}{r_{max}^2}\left[\int_{-L}^{x}\lambda^2(\xi)d\xi + \frac{H(x)}{6}\left(3\lambda^2(x) + H^2(x)\right)\right]\Big|_{h_0}^{h_0+\Delta h} \tag{S41}$$

The linear approximation is applied on the right-hand size of equation (S41). The formula can be expressed as:

$$\Delta s = \Upsilon(\beta,\Lambda,x^*)\cdot\Delta h \tag{S42}$$

$$\Upsilon(\beta,\Lambda,x^*) = \frac{1}{2\pi^2}[\xi^+ - \xi^- cos(\pi x^*)]^2\left\{2 - 2\left[\frac{\Lambda}{\beta}\xi^- cos(\pi x^*)\right]^2 + \left(\frac{\Lambda}{\beta}\right)^2\xi^+\xi^- cos(\pi x^*)\right\}\left[\sqrt{1 + \left[\frac{\Lambda}{\beta}\xi^- sin(\pi x^*)\right]^2} + \frac{\Lambda}{\beta}\xi^- sin(\pi x^*)\right]^2 \tag{S43}$$

The approximation error ε is defined as the ratio of linearized displacement to accurate displacement at the rear meniscus. The linearized displacement is calculated from equation (S42), and the accurate displacement is calculated numerically based on volume conservation. Apparently, ε is function of $\Delta h/h_0$. The approximation error ε with respect to $\Delta h/h_0$ is displayed in Figure S1. The geometric parameters used: $\Lambda = 4$, $\beta = 20$, $x^* = -0.05$. It shows that the error is within 5% for the relative oscillatory amplitude in 50%.

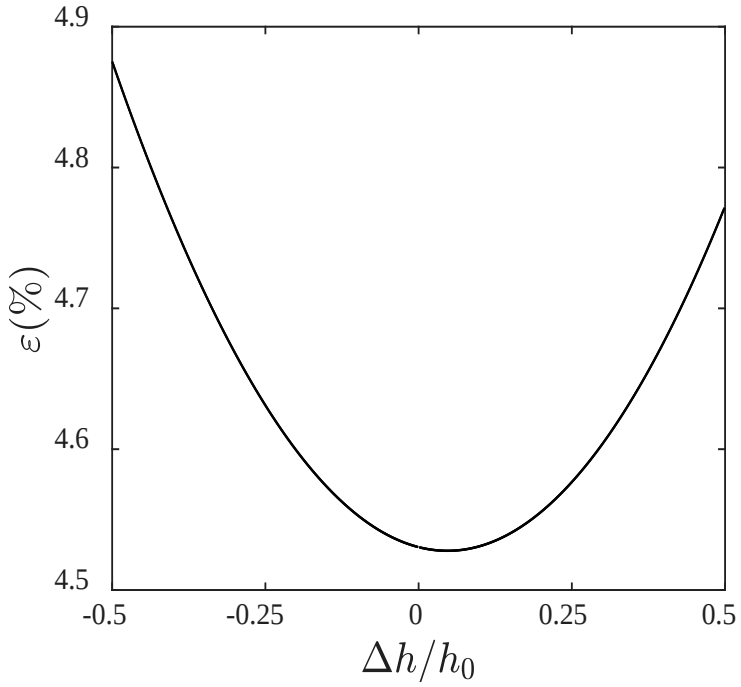

Figure S1. The linear approximation error with respect to dimensionless amplitude of oscillation at front meniscus.

Text S3.

Pressure Differences

In stationary state, the balance of external pressure and capillary pressure is:

$$P_{w1} - P_{w2} = 2\sigma\left[\frac{1}{r_{men}(h_0)} - \frac{1}{r_{men}(s_0)}\right] \tag{S44}$$

In transient state, the net pressure of them is:

$$\Delta P_e - \Delta P_c = 2\sigma\left[\frac{1}{r_{men}(h_0)} - \frac{1}{r_{men}(s_0)}\right] - 2\sigma\left[\frac{1}{r_{men}(h_0+\Delta h)} - \frac{1}{r_{men}(s_0+\Delta s)}\right] \tag{S45}$$

In light of rear meniscus locating in flat wall, $r_{men}(s_0) = r_{men}(s_0 + \Delta s)$. Therefore, equation (S45) can be reformulated as:

$$\Delta P_e - \Delta P_c = 2\sigma\left[\frac{1}{r_{men}(h_0)} - \frac{1}{r_{men}(h_0+\Delta h)}\right] \tag{S46}$$

If the rear meniscus also locates in curved region, the variation of rear meniscus needs to be considered in equation (S46).

The linearized approximation can be applied on equation (S46) to linearize the relation of pressure difference and displacement:

$$\Delta P_e - \Delta P_c = -2\sigma \frac{f(\beta,\Lambda,x^*)}{r_{min}^2}\Delta h \tag{S47}$$

where,

$$f(\beta,\Lambda,x^*) = \frac{\pi^2}{2\beta\Lambda}\frac{-\xi^- sin(\pi x^*)}{[\xi^+ - \xi^- cos(\pi x^*)]^2}\frac{2-2\left[\frac{\Lambda}{\beta}\xi^- cos(\pi x^*)\right]^2+\left(\frac{\Lambda}{\beta}\right)^2\xi^+\xi^- cos(\pi x^*)}{\left[1+\left(\frac{\Lambda}{\beta}\xi^- sin(\pi x^*)\right)^2\right]^{3/2}} \tag{S48}$$

As in appendix A, the approximation error ε is defined as the ratio of linearized pressure difference to accurate pressure difference. The linearized pressure difference is calculated from equation (S47). The accurate pressure difference is calculated from equation (S46). Apparently, ε is function of $\Delta h/h_0$. The approximation error is displayed in Figure S2 for a specific geometry: $\Lambda = 4, \beta = 20, x^* = -0.05$. It shows that the error is within 15% for the relative oscillatory amplitude in 20%.

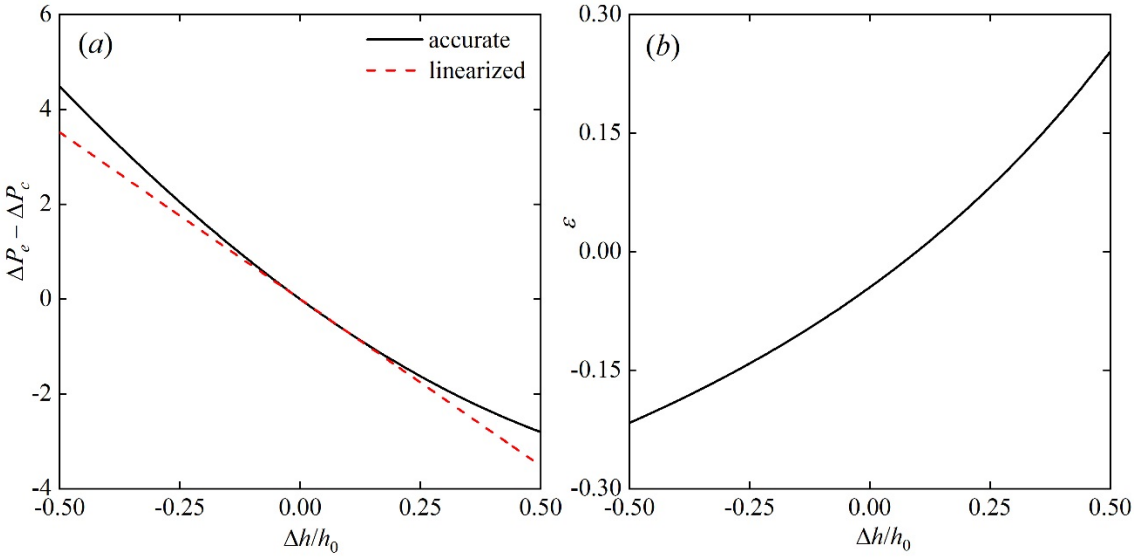

Figure S2. (a) The linearized and accurate pressure difference with respect to dimensionless amplitude of oscillation at front meniscus; (b) the approximation error incurred in the linearized approximation.

Reference

Beresnev, I. A., and W. Deng (2010), Viscosity effects in vibratory mobilization of residual oil, *Geophysics*, *75*(4), N79-N85.

Deng, W., and M. B. Cardenas (2013), Dynamics and dislodgment from pore constrictions of a trapped nonwetting droplet stimulated by seismic waves, *Water Resources Research*, *49*(7), 4206-4218.

Hilpert, M., G. H. Jirka, and E. J. Plate (2000), Capillarity-induced resonance of oil blobs in capillary tubes and porous media, *Geophysics*, *65*(3), 874-883.